Quartz crystal microbalance with dissipation monitoring of supported lipid bilayers on various substrates

Nam-Joon Cho[1,2], Curtis W Frank[2], Bengt Kasemo[3] & Fredrik Höök[3]

[1]Division of Gastroenterology and Hepatology, Department of Medicine, Stanford University, Stanford, California, USA. [2]Department of Chemical Engineering, Stanford University, Stanford, California, USA. [3]Department of Applied Physics, Chalmers University of Technology, Gothenburg, Sweden. Correspondence should be addressed to N.-J.C. (ncho@stanford.edu) or F.H. (fredrik.hook@chalmers.se).

Published online 20 May 2010; doi:10.1038/nprot.2010.65

Supported lipid bilayers (SLBs) mimic biological membranes and are a versatile platform for a wide range of biophysical research fields including lipid–protein interactions, protein–protein interactions and membrane-based biosensors. The quartz crystal microbalance with dissipation monitoring (QCM-D) has had a pivotal role in understanding SLB formation on various substrates. As shown by its real-time kinetic monitoring of SLB formation, QCM-D can probe the dynamics of biomacromolecular interactions. We present a protocol for constructing zwitterionic SLBs supported on silicon oxide and titanium oxide, and discuss technical issues that need to be considered when working with charged lipid compositions. Furthermore, we explain a recently developed strategy that uses an amphipathic, α-helical (AH) peptide to form SLBs on gold and titanium oxide substrates. The protocols can be completed in less than 3 h.

INTRODUCTION

Supported lipid bilayers (SLBs) are a widely accepted model system to mimic the natural cell membrane, the site of many critical biomacromolecular interactions[1]. A lipid bilayer is the backbone of the cell membrane; lipid amphiphilicity shapes the membrane's role as a protective barrier between intra- and extracellular regions because lipids self-assemble into a bilayer that regulates what spontaneously enters and exits the cell[1,2]. As a model system for studying membrane properties and macromolecular interactions, SLBs are extremely versatile because they can be functionalized by, among many other possibilities, changing the lipid composition or incorporating membrane-associated (transmembrane or peripheral) proteins[3]. From a basic science perspective, the design of these platforms is also important for understanding membrane properties. Researchers are applying knowledge about these properties (e.g., electrical surface change[4,5], ion conductance, lateral fluidity[6] and domain formation[7]) to engineer novel sensor technology based on molecular recognition events such as biomacromolecule-substrate-binding interactions[3,8–10]. By studying biomacromolecular interactions with a model membrane system, one can also develop increasingly sophisticated biomedical assays for applications such as drug screening and medical diagnostics[3,10–14]. Yet another application of growing interest is functionalized membranes as substrates for cell culture[15].

Surface-mediated vesicle fusion is a popular technique to form SLBs[16]. McConnell and co-workers[17] were the first group to report the fabrication of an SLB by vesicle fusion on a hydrophilic substrate; however, they did not determine the kinetic pathway of the formation process. Fluorescence recovery after photobleaching experiments have shown that SLBs formed by this method are continuous and that constituent lipids have a lateral fluidity not very different from that of native cell membranes[17,18]. Atomic force microscopy (AFM) has also been used to monitor bilayer formation at different stages of the process, elucidating critical morphological information about the self-assembly process[19]. However, AFM measurements, even in noncontact mode, are affected by tip–substrate interactions and it is quite difficult to measure changes in the thin film properties of an SLB on short time scales with scanning probe techniques. By comparison, a host of acoustic- and optical-based sensor techniques, including surface plasmon resonance (SPR)[20,21], ellipsometry[22,23], reflectometry[24,25] and quartz crystal microbalance with dissipation monitoring (QCM-D)[26], can quantitatively monitor changes in film thickness and mass without the addition of external labels. By combining the information gained using these techniques, the user can identify interesting events in kinetics, such as the rate of vesicle binding, point of critical vesicle coverage before rupture and completed SLB formation. Among these spectroscopic techniques, QCM-D uniquely captures the film's mass and energy-dissipating properties, making it particularly useful for probing changes in viscoelastic properties during film formation. This measurement capability is especially important for SLB characterization, in which the viscoelastic properties of the resultant bilayer and its intermediate state—an incomplete layer of adsorbed, unruptured vesicles—differ significantly.

With regard to SLB formation, QCM-D can monitor the real-time kinetics of the vesicle fusion process and characterize the platform's mass and viscoelastic properties[27–34], as described in **Figure 1**. In addition, the technique can monitor SLB's interaction with other biomacromolecules such as proteins and drugs[11,35]. Furthermore, the QCM-D measurement principles enable a wide range of substrate possibilities for SLBs, depending on experimental needs[36]. In this protocol, we first introduce newcomers to the methods for forming SLBs of different lipid compositions on two popular substrates, silicon and titanium oxides. In addition, we discuss how an amphipathic, α-helical (AH) peptide can be used to form zwitterionic SLBs on gold and titanium oxide substrates, allowing researchers to take advantage of these materials' attractive properties. In the absence of AH peptide, zwitterionic lipid vesicles typically adsorb intact on gold and titanium oxide, resulting in the formation of a monolayer of unruptured vesicles[37,38]. This modified protocol gives researchers greater freedom over lipid composition

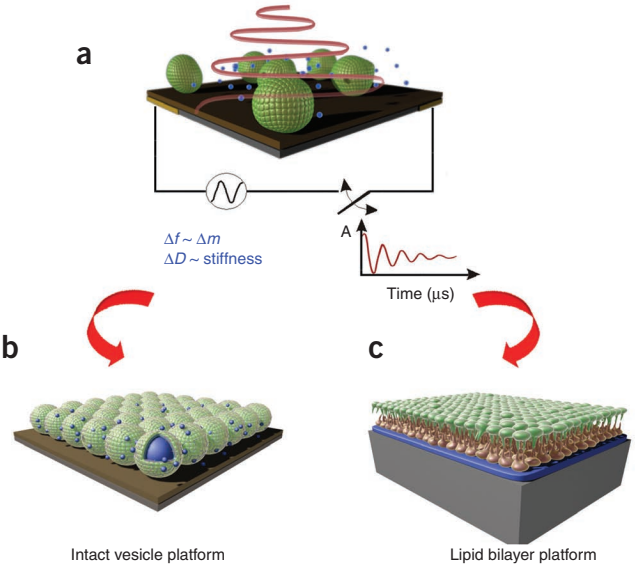

Figure 1 | Quartz crystal microbalance with dissipation (QCM-D)-monitoring principles. (**a**) Schematic representation of the QCM-D principle. The spheres correspond to unruptured vesicles adsorbed onto the substrate. The blue balls correspond to acoustically coupled solvent. The quartz crystal substrate is positioned between two electrodes. Because quartz is a piezoelectric material, the crystal oscillates when an AC voltage is applied across it. When additional mass (e.g., lipid vesicles and coupled solvent) adsorbs onto the substrate, the resonance frequency of oscillation decreases. The frequency change, Δf, is proportional to the mass of the adsorbed material including coupled solvent. When the circuit is opened, the crystal's oscillation will decay exponentially. The energy loss per stored energy during one oscillation cycle is referred to as energy dissipation, D, which is proportional to $1/\tau$, where τ is the decay time constant. Films with large viscous loss will display larger ΔD than more rigid films because the ratio between energy loss and stored energy will be larger. The inset shows a typical oscillation decay as a function of time after the circuit is opened. (**b**) A monolayer of adsorbed, unruptured vesicles can be formed on a number of substrates including gold and titanium oxide. (**c**) A supported lipid bilayer platform can be formed on a silicon oxide substrate through surface-mediated vesicle fusion.

and substrate choices, and leads to new applications in a diverse set of fields including nanoplasmonics[39–42], semiconductor devices[43] and medical implant surfaces[44]. With this new method for forming SLBs on gold surfaces, there is also great potential for the design of more sophisticated electrophysiological biosensors[3,11,35].

Criteria for experimental materials

Three main factors contribute to vesicle fusion on solid substrates: membrane tension[45], vesicle–substrate and vesicle–vesicle interactions[37,38]. To form complete SLBs with minimal defects in a reproducible manner, two of the most important parameters to be controlled are the membrane tension of the vesicles and vesicle lamellarity. It is recommended to work with small unilamellar vesicles (SUVs) with a monodisperse size distribution that has an average diameter of less than 90 nm; vesicles of such size should have sufficient membrane tension for fusion to be efficient[45]. Although vesicle fusion depends on additional factors such as lipid composition and surface chemistry, larger vesicles in general may not have sufficient membrane tension to cause spontaneous vesicle rupture[46,47].

There are two popular methods to generate SUVs. The first is the sonication method (either high-power bath or tip sonication), which uses ultrasonic energy waves to induce fragmentation and collisions between large multilamellar vesicles. The vesicle structures are disrupted and the resulting small aggregates rearrange into SUVs[48–51]. The extrusion method is the other technique; vesicle size distribution is reduced as vesicles are mechanically extruded through a polycarbonate track-etched membrane with defined pore sizes[52]. The extrusion technique also forms SUVs if the vesicle solution is passed through the membrane multiple times (preferably >23 times). For a detailed protocol regarding SUV preparation by these methods, refer to references 52,53. Standard buffers that approximate biological conditions (pH 7–7.5, $I = 0.15$–0.2 M) produce excellent results. The data in **Figure 2** were obtained with a Tris buffer (10 mM Tris, 150 mM NaCl (pH 7.0)). In addition to reducing size, membrane tension can be increased by creating an osmotic pressure difference between the vesicle interior and the solution[54]. Vesicles should, in this case, be prepared preferably in Milli-Q water and then subsequently diluted in buffer before use within 30 min.

Preparation of zwitterionic SLBs on a silicon oxide substrate

The QCM-D technique was first used to study vesicle interactions with solid substrates by Keller and Kasemo[37]. They showed that vesicles can interact with solid substrates by either adsorbing irreversibly while remaining intact or forming a supported lipid monolayer or bilayer[37], depending on the substrate's properties. On the basis of this original work, along with more recent studies[3,11,26,35,37,38,55,56], it has been shown that vesicles have an attractive interaction with silicon oxide[37], silicon nitride[57], titanium oxide[58], oxidized Pt[59], oxidized Au[37] and alkanethiol[37] and phosphate/sulfate-thiol-modified[60] Au substrates, although the outcome of the interaction (adsorbed intact vesicles, continuous SLB or a mixture of these two) depends on bulk properties[60], lipid composition[61–64] and the substrate's physical[65] and chemical properties[37].

Because of QCM-D's ability to monitor in real time the mass and viscoelastic property changes related to vesicle–substrate interactions, the technique has revealed that vesicle fusion on solid substrates follows a general two-step mechanism[37], at least in the case of zwitterionic lipid vesicles. QCM-D studies have revealed that the detailed vesicle fusion kinetics depend on factors including osmolality, temperature, flow rate, vesicle concentration, vesicle lipid composition and the substrate's surface chemistry[58,66,67].

On the basis of the classical two-step spontaneous SLB formation mechanism on a silicon oxide substrate, vesicles first adsorb irreversibly to the substrate. By themselves, vesicle–substrate interactions are generally insufficient to promote individual vesicle rupture[37,38]. Therefore, a critical coverage of adsorbed vesicles must be reached before vesicle fusion begins (**Fig. 2**). At this concentration, the combination of vesicle–vesicle and vesicle–substrate interactions promotes vesicle fusion, most likely through local vesicle rupture into SLB patches, the edges of which promote an autocatalytic SLB formation process[26]. These steps have served as the basis for Monte Carlo simulations that sought to better understand the kinetic pathway of vesicle adsorption, rupture and fusion[68–70]. As indicated in **Figure 2**, frequency (Δf) and dissipation (ΔD) changes are maximized at the critical vesicle coverage. Intact vesicle adsorption results in a viscoelastic film (large dissipation increase) because of a combination of the nonrigid nature of the vesicles and solvent coupled within and between

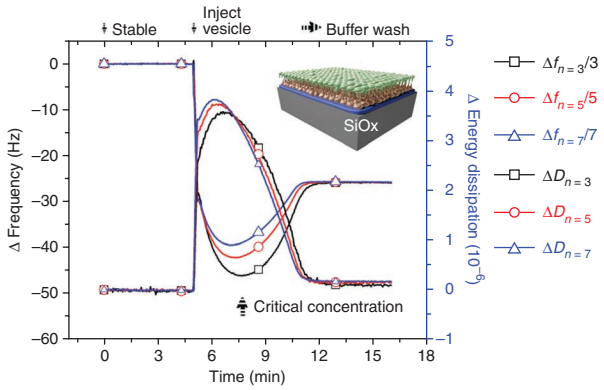

Figure 2 | QCM-D monitoring of zwitterionic SLB formation on a silicon oxide substrate. After the baseline buffer measurement stabilized, POPC vesicles (0.1 mg ml^{-1}) were injected at 5 min, leading to rapid adsorption on the substrate and a corresponding frequency decrease in and dissipation increase at all overtones (n = 3, 5 and 7). As indicated by maximum changes in the frequency and dissipation responses, the critical vesicle coverage was reached at 8 min. Thereafter, vesicles began to rupture on the substrate, forming an SLB. The frequency and dissipation values stabilized at approximately −25 Hz and ~0.1 × 10^{-6}, respectively. Data at multiple overtones (n = 3–7) are presented to show typical deviations for viscoelastic films, such as adsorbed, unruptured vesicles (see frequency and dissipation responses at the point of critical vesicle coverage). The inset is an illustration of an SLB supported on silicon oxide.

the vesicles. The negative frequency shift indicates the addition of mass, which decreases the crystal's resonance frequency of oscillation. Initial vesicle rupture creates patches of bilayer with hydrophobic edges, which propagate continued vesicle rupture until the lipid bilayer is complete and the edges are minimized. After bilayer formation, the dissipation value returns to nearly zero, which indicates that the bilayer is 'rigid' (compared with 'soft' vesicles) and has a low amount of bound solvent, and the frequency shift is reduced because of a loss of solvent trapped inside vesicles, in spite of the fact that there is a net addition of lipid mass also after the maximum frequency and dissipation shift[37]. The net addition of lipid mass after the peaks in Δf and ΔD was verified by simultaneously combining QCM-D with SPR21 and optical reflectometry[25].

Furthermore, the frequency and dissipation response kinetics can be modeled to better understand the property changes of the film, giving an insight into structural transformation. Bilayer thickness (~5.0 nm) can be determined from the change in frequency using the Sauerbrey relationship:

$$\Delta m = -C_{\mathrm{QCM}} \frac{\Delta f_{\mathrm{n}}}{n} \qquad (1)$$

where Δm is the adsorbed mass on the surface, C_{QCM} is the mass sensitivity constant (17.7 ng cm^{-2} Hz^{-1} at f = 5 MHz) and Δf_{n} is the change in the resonance frequency at the nth harmonic. However, the Sauerbrey relationship is only valid for acoustically rigid films (e.g., SLBs) with low dissipation[71]. Therefore, it is important to use a viscoelastic model such as the Voigt-Voinova model to quantify the changes in mass and effective viscoelastic properties of the film during the transformation process from adsorbed vesicles to an SLB[72]. At the critical vesicle coverage in **Figure 2**, the measured responses are characterized by a large dissipation ($\Delta D/\Delta f > 1 \times 10^{-8}$ Hz^{-1}), and both the frequency and dissipation responses display overtone dependencies that are characteristic of acoustically nonrigid films. A viscoelastic model extends QCM-D responses to include the effective viscoelastic properties that cause this overtone dependence. By using such a model, the changes in film thickness, effective shear viscosity and elasticity throughout the entire vesicle-to-bilayer transformation process can be determined. It is important to emphasize, however, that the physical origin of the energy dissipation for adsorbed vesicles most likely stems from a combination of the vesicles' intrinsic properties and the nature of their attachment to the surface[73].

Variations of charged DOPC/DOPS and DOPC/DOEPC SLBs on a silicon oxide substrate

Overall, the formation of charged SLBs follows the same self-assembly process as zwitterionic SLBs[63,64]. However, it is important to note that vesicle–substrate interactions can vary significantly and may require a fine-tuning of the protocol. When working with vesicles composed of 1,2-dioleoyl-sn-glycero-3-phosphocholine (DOPC) and 1,2-dioleoyl-sn-glycero-3-[phospho-L-serine] (DOPS) lipid mixtures, there are repulsive interactions between negatively charged vesicles (DOPS has a negatively charged head group) and the negatively charged silicon oxide substrate[22] (**Fig. 3a–c**). This results in a higher critical vesicle coverage before the start of vesicle rupture. To improve the conditions to favor vesicle rupture and SLB formation, one may include calcium in all buffers after the extrusion process when working with negatively charged vesicles[74]. Recent studies have shown that magnesium ions display a similar, and even stronger, promotion of bilayer formation[54]. Divalent cations trigger bilayer formation by bridging the interaction between the phosphatidylserine lipid head groups and the negatively charged substrate[74]. Instead of using a divalent cation to stabilize the otherwise repulsive vesicle–substrate interactions, the negatively charged SLBs in **Figure 3** were formed by using a Tris buffer with 250 mM NaCl instead of 150 mM NaCl. This increase in osmotic pressure was sufficient to form complete, negatively charged SLBs without the addition of a divalent cation (**Fig. 3a–c**)[64]. With regard to the formation of charged SLBs as a function of salt concentration, we have conducted these studies previously and have noted that an increase in osmotic pressure leads to faster SLB formation kinetics. Therefore, when working with negatively charged vesicles, we recommend a higher osmotic pressure gradient to counter the effects of more repulsive electrostatic interactions between vesicles and the substrate as one method presented in this protocol.

When working with DOPC/1,2-dioleoyl-sn-glycero-3-ethylphosphocholine (DOEPC) vesicles (**Fig. 3d–f**), SLB formation kinetics will have only one step (i.e., spontaneous fusion occurring immediately after vesicle adsorption)[19]. This is due to an attractive electrostatic attraction between the positively charged vesicles (DOEPC has a positively charged head group) and the negatively charged substrate, which makes vesicle–substrate interactions sufficient by themselves to cause vesicle rupture. Thus, a critical coverage of adsorbed vesicles on the substrate is not necessary to induce spontaneous vesicle rupture. The electrostatics favor individual vesicle rupture. In this case, there is no frequency minimum and only a very minor dissipation maximum before SLB formation. It is important to note that the final resonance frequency change

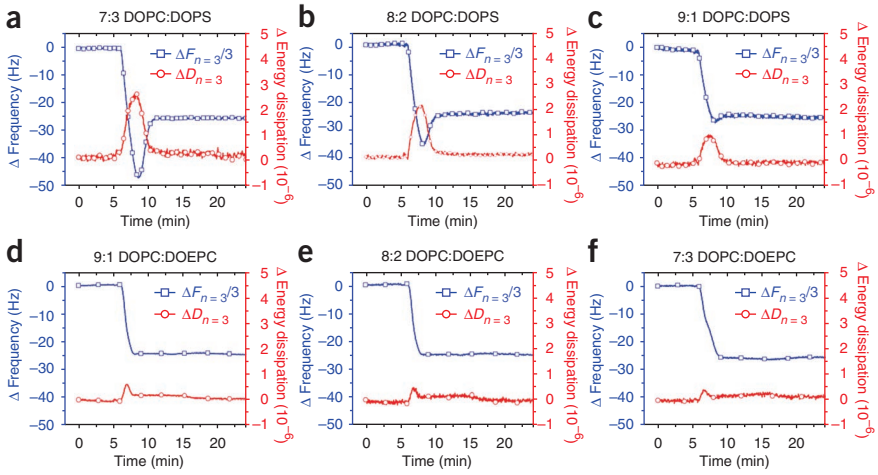

Figure 3 | QCM-D monitoring of charged SLB formation on a silicon oxide substrate. (**a**–**f**) After the buffer measurement stabilized, the respective vesicle solutions (0.1 mg ml^{-1}), 7:3 DOPC:DOPS (**a**), 8:2 DOPC:DOPS (**b**), 9:1 DOPC:DOPS (**c**), 9:1 DOPC:DOEPC (**d**), 8:2 DOPC:DOEPC (**e**), and 7:3 DOPC:DOEPC (**f**), were injected at 5 min. After SLB formation, a buffer wash was performed. All final frequency and dissipation values were in the range of -25 ± 1 Hz and $<0.15 \times 10^{-6}$, respectively. All data presented were measured at the third overtone.

for a DOPC/DOEPC SLB can be lower than the value discussed above. A frequency shift of -24.0 ± 1.0 Hz, rather than -25.0 ± 1.0 Hz, is a better estimate of the final value for a complete, positively charged SLB, likely due to a difference in lipid–substrate interactions. We believe that the frequency shift difference is due to a reduced water layer between SLB and the solid support. Both of our research groups have routinely noticed this value and it is well documented in literature. On the basis of our preliminary studies to better understand this value, we believe that the thinner water layer between the SLB and the solid support is caused by stronger electrostatic interactions between the positively charged SLB and the negatively charged solid support.

Preparation of negatively charged SLBs on a titanium oxide substrate by divalent calcium cation

Titanium oxide has a number of attractive properties such as biocompatibility and a high refractive index that make it suitable for medical implant[75] and analysis using optical waveguide lightmode spectroscopy[76], which offers a high measurement sensitivity to film birefringence[77]. However, the formation of SLBs on titanium oxide is not as straightforward as on silicon oxide. Rossetti *et al.*[61,62] reported that the divalent calcium cation can promote the spontaneous SLB formation of phosphatidylserine-containing vesicles. They concluded that the calcium-mediated short-range attraction between vesicles and the substrate may result from the cation bridging the charged groups, as in the case described above for forming negatively charged SLBs on silicon oxide. A related finding was also reported by Richter *et al.*[78] who discussed the influence of lipid redistribution on the vesicle fusion process. Using calcium to stabilize vesicle–substrate interactions, we show in **Figure 4** of this protocol the formation of a negatively charged SLB containing a mixture of POPC and a pyrophosphate lipid, which has a double-negatively charged head group. In the absence (**Fig. 4a**) or presence (**Fig. 4b**) of calcium, vesicles either adsorb and remain intact, or eventually rupture to form an SLB, respectively. This protocol is suitable for forming negatively charged SLBs that contain different anionic lipids on titanium oxide. Although negatively charged lipids may be preferentially oriented toward the substrate, it is important to point out that calcium in combination with negatively charged lipids is required to form SLBs on titanium oxide; this procedure is not suitable for forming single-component zwitterionic SLBs on titanium oxide.

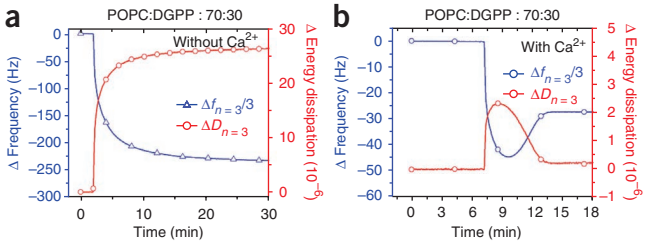

Figure 4 | QCM-D monitoring of negatively charged SLB formation on a titanium oxide substrate induced by divalent calcium cation. After the baseline buffer measurement stabilized, the vesicle solution (0.1 mg ml^{-1}) was injected at 10 min. (**a**) In the absence of calcium, vesicles only adsorbed onto the substrate but did not rupture to form an SLB. (**b**) In contrast, the addition of calcium stabilized the vesicle–substrate interactions, resulting in SLB formation.

Preparation of zwitterionic SLBs on gold and titanium oxide substrates by an amphipathic, AH peptide

Supported lipid bilayer formation requires the substrate to have specific properties, particularly, hydrophilicity and surface charge density, which help promote vesicle deformation and subsequent rupture into a continuous SLB[37]. Despite not possessing favorable surface properties for vesicle fusion, titanium oxide and gold are two attractive substrate candidates because of their respective biocompatibility[55] and electrical properties[79]. The electrical properties of gold are especially advantageous as they can be used to take advantage of the SLB's insulating properties for ion conductance–based sensor measurements[43]. To overcome these surface-dependent constraints, a new method was recently developed to form a zwitterionic lipid bilayer on these substrates. In this method, an amphipathic, AH peptide is used as a vesicle-destabilizing agent. This process results in the formation of continuous SLBs on gold and titanium oxide surfaces[11,35].

As presented in **Figure 5**, vesicles first adsorb irreversibly to the substrate while remaining unruptured (**Fig. 5a**). When an AH peptide derived from a hepatitis C virus protein[10] is added, it destabilizes the vesicle structures by a presumed electrostatic interaction. The vesicles then expand and eventually rupture, forming an SLB with final frequency and dissipation response values of 25 ± 0.5 Hz and $<0.1 \times 10^{-6}$, respectively (**Fig. 5b**). We define this structural transformation as *AH peptide-induced vesicle fusion*, as the main driving force for vesicle rupture and subsequent SLB formation is the vesicle interaction with AH peptide[26].

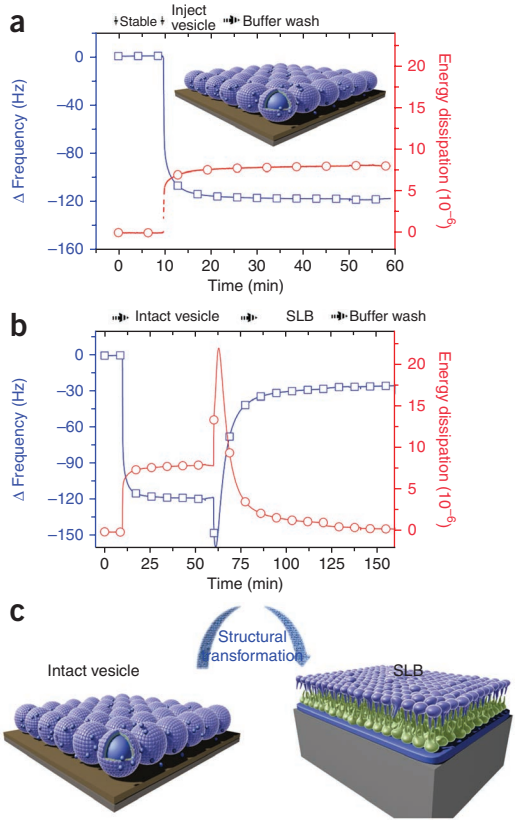

Figure 5 | QCM-D monitoring of AH peptide-mediated structural transformation from intact vesicles to an SLB on a gold substrate. (**a**) After the baseline buffer measurement was stabilized, POPC vesicles (0.1 mg ml^{-1}) were injected at 5 min. The vesicles adsorbed onto the substrate and formed a layer of unruptured vesicles. After the formation of a layer of unruptured vesicles, a buffer wash was performed. The final frequency and dissipation values were −120 Hz and 8×10^{-6}, respectively. (**b**) After forming the layer of vesicles as given in **a**, an AH peptide solution (13 μM) was added. The AH peptides caused vesicle swelling and subsequent rupture, leading to SLB formation. The SLB had final frequency and dissipation values of −25.5 Hz and 0.08×10^{-6}, respectively. (**c**) A schematic representation of the AH peptide-mediated structural transformation from adsorbed, intact vesicles to an SLB.

By using a viscoelastic model such as the Voigt-Voinova model, we can better understand the structural transformation (**Fig. 5c**) in terms of changes in film thickness and effective viscoelastic properties[35]. The resulting thicknesses of the bilayer calculated using both the Sauerbrey and Voigt-Voinova models are in good agreement as long as $\Delta D/\Delta f < 1 \times 10^{-8}$ Hz^{-1}. This indicates that the structural transformation from unruptured vesicles to continuous SLB that is induced by the AH peptide results in an acoustically rigid lipid bilayer[35]. Although the mechanism of SLB formation differs on silicon oxide compared with gold and titanium oxide, the end result is equivalent: a zwitterionic SLB with identical mass and viscoelastic properties. We have confirmed that AH peptide does not contribute additional mass to the supported bilayer[11,24,26,54,73], and the result is a complete SLB with minimal defects.

To better analyze biomacromolecular interactions at solid interfaces, QCM-D can be combined with other advanced microscopy and spectroscopy techniques such as AFM[19,74], fluorescence microscopy[80], fluorescence recovery after photobleaching[81], SPR[21], ellipsometry[23], electrical impedance spectroscopy[82] and optical reflectometry[77]. As the QCM-D measurement principle is acoustic based, it measures total adsorbed mass including coupled solvent. In contrast, optical-based techniques such as SPR, ellipsometry and optical reflectometry only measure responses that, to a first approximation, are proportional to the mass change associated with adsorbed, nonsolvent molecules. By combining QCM-D with these optical techniques, the coupled solvent mass can be calculated to better understand how a hydrodynamically coupled solvent is related to structural transformations[24].

An overview of the procedure

In this protocol, we have described a number of suitable protocols, along with tips and tricks to form complete SLBs of various charged lipid compositions on silicon oxide, titanium oxide and gold, all of which are compatible with many surface-based techniques, including QCM-D monitoring. Although the parameters we provide are excellent for SLB formation, every research group has a different reason for using an SLB platform and this may require the use of different materials or conditions. On the basis of the initial QCM-D response in buffer, a complete SLB formation should in general correspond to a frequency change of -24 ± 1.5 Hz and a dissipation change of less than 0.2×10^{-6}. Note that these frequency and dissipation changes are only valid when using the same buffer. For example, if one records the initial measurement in Tris/NaCl no. 1 buffer and then analyzes the QCM-D response to SLB formation in Tris/NaCl no. 2 buffer, the frequency and dissipation changes will not agree with the values listed above. This is because of changes in solution viscosity, which influences the QCM-D response. Thus, it is important to analyze the QCM-D response in the same buffer as the initial measurement. In addition to single-component, zwitterionic SLBs on silicon oxide, we stress that negatively charged SLBs can be formed on titanium oxide by the addition of divalent ions such as calcium. Furthermore, we describe an additional protocol that uses an AH peptide to destabilize adsorbed, unruptured vesicles, resulting in the formation of a zwitterionic SLB on both gold and titanium oxide substrates. The latter protocol also holds great promise for the formation of planar SLBs from biological membrane extracts, which would further extend the applicability of such membrane platforms to new disciplines. It is noteworthy that, although the incorporation of functional transmembrane proteins has been difficult, it is still one possibility to functionalize SLBs. Our key point is that SLBs can be functionalized with membrane-associated proteins and it is up to the user to design a more complex biomimetic platform that fits their specific interests. In this protocol, we are interested in presenting one basic platform—a model membrane composed of phospholipids on various substrates—for researchers to take advantage of.

Note that the data shown for these protocols have been obtained with a Q-Sense E4 series (Q-Sense AB, Sweden) instrument, which is equipped with a pump flow control system. However, the protocols are compatible with other systems using batch-mode measurements, such as the Q-Sense D300 series (Q-Sense AB), and alternative surface-sensitive methods (see above)[83].

MATERIALS

REAGENTS

- Milli-Q water (>18 MΩ cm)
- 1-palmitoyl-2-oleoyl-sn-glycero-3-phosphocholine (POPC), 1,2-dioleoyl-sn-glycero-3-phosphocholine (DOPC), 1,2-dioleoyl-sn-glycero-3-[phospho-L-serine] (DOPS), dioleoylglycerol pyrophosphate (DGPP) and 1,2-dioleoyl-sn-glycero-3-ethylphosphocholine (DOEPC) lipids (Avanti Polar Lipids) **! CAUTION** The protocol is based on a vesicle solution with a lipid concentration of ~0.1 mg ml^{-1}. It is recommended to initially prepare vesicle solution at a higher concentration of 1–5 mg ml^{-1} with ease and then subsequently dilute with buffer before the experiment. However, the extrusion process for sizing vesicle populations does not in general work as well for vesicle solutions at lipid concentrations greater than 10 mg ml^{-1}.
- 200 proof ethanol
- Analytical grade Tris buffer, NaCl, $CaCl_2$ and sodium dodecyl sulfate (SDS)

EQUIPMENT

- Plasma Prep 5 Plasma Cleaner (GaLa Instrumente GmbH)
- Quartz Crystal Microbalance with Dissipation Monitoring (QCM-D) D300, E1 or E4 system (Q-Sense AB)
- Reglo Digital M2-2/12 Peristaltic Pump (Ismatec) [only for QCM E series models]
- QCM crystals with silicon oxide, titanium oxide and gold coatings (Q-Sense AB)
- Syringe filters (0.2 μm, Nalgene)

REAGENT SETUP

Solutions Prepare the following aqueous solutions for SLB formation: Tris/NaCl no. 1 (10 mM Tris, 150 mM NaCl (pH 7.0)), Tris/NaCl no. 2 (10 mM Tris, 250 mM NaCl (pH 7.0)) and Tris/NaCl no. 3 (10 mM Tris, 150 mM NaCl, 5 mM $CaCl_2$ (pH 7.0)). Filter all Tris buffers with a 0.2-μm membrane before use. For cleaning the QCM-D system, prepare a 0.1-M SDS solution.

EQUIPMENT SETUP

Quartz crystals Rinse crystals thoroughly with water and ethanol and then dry with nitrogen air. Remove any organic contaminants from the substrate by plasma cleaning (with substrate facing up) at 75 W for 3 min. Use crystals immediately after plasma cleaning for best results. We used a house-built UV/ozone system with specific wavelengths of 185 and 254 nm. After plasma cleaning, the typical contact angle of the substrates should be as follows: $SiO_2 \leq 10°$, $TiO_2 \leq 20°$ and Au ≤ 35°.

QCM-D E1 or E4 flow cells and tubing Clean the system while all of the tubing is connected and quartz crystals are in the flow cells. Rinse the system with a 0.1 M SDS solution, water and finally with ethanol at a high flow rate of 1 ml min^{-1}. Continue rinsing for at least 10 min per liquid. After rinsing with the liquids, dry the tubing and flow cells by turning the pump on, without solvent, at the same flow rate for 2 min. Do not dry completely because crystals will become firmly attached to the rubber O-rings and can possibly crack when being removed. After cleaning, detach the setup (tubing and flow cells) and dry each flow cell with a gentle stream of nitrogen air.

QCM-D D300 axial flow chamber Alternatively, the QCM-D D300 instrument can be used. The only difference between the D300 and E series is flow control. The D300 is a batch system, whereas the E series involves continuous flow. For cleaning, ensure that a crystal is mounted in the measurement chamber to prevent electrical damage. First, turn the control valve to the 'loop out' position and flow at least 10 ml of the 0.1 M SDS solution through the reservoir chamber. Thereafter, close the valve and allow the SDS solution to soak for at least 10 min. Repeat with water and then ethanol. Next, turn the valve to the 'sensor out' position and repeat the cleaning procedure in order to clean the measurement chamber in the same manner. After washing, disconnect the D-300 setup and remove the crystal. Dry all tubing with a gentle stream of nitrogen air.

PROCEDURE

1| Immediately mount the quartz crystal in the flow cell after plasma cleaning and attach the cell module to electrical contacts.

▲ CRITICAL STEP During the crystal mounting process, ensure that the crystal is dry. Moreover, place the crystal in a dry environment before use to prevent any humidity effects. Any wetness on either electrode will affect the initial frequency and dissipation measurements.

2| Run the QSoft program and activate temperature control at the desired temperature (24 °C) to minimize the thermal drift that will affect measurement values. For the D-300, adjust the setpoint temperature to about 1 °C above the ambient temperature.

3| Obtain the crystal's resonance frequency and dissipation values in air at several overtones. Typical resonant frequency and dissipation values are summarized in **Table 1** (ref. 65). In addition, we summarized the second signature, S_2, values ($S_2 = \Delta f/N\Delta D$) that can be used as an initial check to verify proper crystal mounting and instrument performance. The ratio of the frequency change divided by the product of the harmonic number and the dissipation change defines S_2. For more information, please refer to reference 54.

▲ CRITICAL STEP Ensure that resonance frequencies as shown in **Table 1** for typical values are checked. Each harmonic's resonance frequency should be in multiples of 5 MHz, such that 5 MHz corresponds to the fundamental frequency, 15 MHz for the third overtone and so on. Note that there is a slight deviation of S_2 for the fundamental resonance frequency.

4| Start the peristaltic pump and flow Tris/NaCl no. 1 buffer into the system at a flow rate of 250 μl min^{-1}. For the D-300, turn the control valve to the 'loop out' position and allow ~1.5 ml of buffer liquid to flow through the system. Thereafter, change the knob to the 'sensor out' position and allow the buffer to enter the measurement chamber. After fully exchanging solutions (minimum of 1 ml), turn the valve to the 'close' position.

▲ CRITICAL STEP The typical values of Δf and ΔD in both air and solution are summarized in **Table 1**. Given the deviations between these values, it is essential to prevent air bubbles from entering the measurement chamber for the successful completion of the experiment. If there are air bubbles in the D-300's reservoir, rinse thoroughly with more liquid (first turn

TABLE 1 | Summary table of S_2 signature.

	Air		Solution		Air to solution			Signature
Frequency (MHz)	Fre (Hz)	D (10^{-6})	Fre (Hz)	D (10^{-6})	Δf (Hz)	ΔD (10^{-6})	Overtone	S_2 (10^6)
15	14,874,981	14.77	14,873,804	175.16	1,177	160.39	3	2.45
25	24,788,268	10.91	24,786,741	133.17	1,527	122.26	5	2.50
35	34,700,076	8.58	34,698,313	109.69	1,763	101.11	7	2.49
45	44,612,500	7.59	44,610,510	97.97	1,990	90.38	9	2.45
55	54,524,749	10.26	54,522,542	91.91	2,207	81.65	11	2.46
65	64,437,606	10.04	64,435,180	85.54	2,426	75.5	13	2.47

D, dissipation; Fre, frequency.

The typical values of resonance frequency and dissipation obtained from the QCM-D measurements in air and solution (water or buffer solution) at six harmonics are presented. The second signature, S_2, defines the ratio of the resonance frequency change divided by the product of the harmonic number and the dissipation change and can be used as an initial check of the system's performance [10,11,35,65,80,85–88].

the control valve to the 'loop out' position and gently tap the inlet tubing and reservoir with a finger) until the bubbles pass through and exit the reservoir chamber. Note that the values in solution can vary slightly depending on the solution's ionic strength.

5| Check the resonant frequency and dissipation values in liquid.

▲ **CRITICAL STEP** There are many different causes for error when measuring f and D values. If the resonance frequency and dissipation values are off by more than 20%, check for tube leakages, air bubbles, large substrate defects (e.g., cracks), pressure changes (e.g., uneven mounting), backside reactions and O-ring swelling (e.g., reaction with organic solvent).

6| Start the measurement and allow the buffer to flow for 10 min. Once the frequency and dissipation values stabilize, stop the pump. For D-300, exchange buffers in the measurement chamber at least twice. Allow the values to stabilize until the change in frequency is less than 1 Hz in 10 min and the change in dissipation is less than 0.2×10^{-6} in 10 min. Note that typical stabilization time periods with proper operation and cleaning should be around 10 min for the E series systems and 30 min for D-300.

▲ **CRITICAL STEP** Although it requires additional time, there are several reasons to flow an excess amount of buffer through the measurement chamber, which include getting rid of entrapped air bubbles in the measurement chamber and tubing, cleaning the tubing and allowing the ion concentration to stabilize on the measurement surface. In addition, any tubing leaks can be identified before the main part of the experiment.

7| After stabilization, restart the measurement and stabilize the signal for at least another 5 min.

8| For formation of zwitterionic and charged SLBs on a silicon oxide substrate (timing, ~1 h), follow the steps in option A. For the formation of negatively charged SLBs on titanium oxide substrate (timing, ~1 h), follow the steps in option B. For the formation of zwitterionic SLBs on gold substrate induced by AH peptide (timing, ~3 h), follow the steps in option C.

(A) Formation of zwitterionic and charged SLBs on a silicon oxide substrate ● **TIMING ~1 h**

(i) Once all the values have stabilized, add ~0.1 mg ml^{-1} vesicle solution (diluted in Tris/NaCl no. buffer) at a flow rate between 100 and 250 µl min^{-1}. A slower flow rate and lower vesicle concentration will show two-step kinetics for SLB formation.

! **CAUTION** A higher flow rate and higher vesicle concentration (>0.5 mg ml^{-1}) may cause the process to occur with one-step kinetics.

(ii) For the D-300, vesicle injection refers to an exchange of the solution in the measurement chamber. Ensure that enough volume (1 ml) is passed through the measurement chamber so that a complete exchange takes place.

(iii) Continue flowing the vesicle solution into the measurement chamber for at least 5 min to ensure that the bilayer is defect free. Thereafter, wash the bilayer with Tris/NaCl no. 1 buffer at a flow rate of 100 µl min^{-1} for 5 min.

▲ **CRITICAL STEP** Flow the buffer continuously to check the integrity of the bilayer and wash out adsorbed vesicles on top of the substrate. If the change in frequency value increases above −23 Hz, repeat Step 8 and add additional vesicle solution to reduce potential SLB defects.

(iv) Wash the bilayer with Tris/NaCl no. 2 buffer at a flow rate of 100 µl min^{-1} for 5 min. The change in osmotic pressure will increase the likelihood of rupturing any adsorbed, intact vesicles.

(v) Wash again with Tris/NaCl no. 1 buffer at a flow rate of 100 μl min^{-1} for 5 min. After washing, the final resonance frequency and dissipation values should be −24.5 ± 1.5 Hz and less than 0.2 × 10^{-6}, respectively.

(B) Formation of negatively charged SLBs on titanium oxide substrate ● **TIMING ~1 h**

(i) Follow the procedure described above up to Step 6.

(ii) Once all the frequency and dissipation response values have stabilized, add ~0.1 mg ml^{-1} vesicle solution (POPC:DGPP (70:30) diluted in Tris/NaCl no. 3 buffer) at a flow rate between 100 and 250 μl min^{-1}. A slower flow rate and lower vesicle concentration will show two-step kinetics for SLB formation. A higher flow rate and higher vesicle concentration (>0.5 mg ml^{-1}) may cause the process to occur with one-step kinetics.

! CAUTION Alternatively, one can also form the bilayer using other negatively charged lipid head groups as long as the anionic lipid percentage is in the range of 15–30%. When selecting lipids, ensure that they have a gel–fluid phase transition temperature well below the experimental temperature range.

▲ CRITICAL STEP When one injects the vesicle solution, it is necessary to use the calcium-containing buffer (Tris/NaCl no. 3). However, do not prepare charged vesicles in this buffer because it will promote vesicle aggregation.

(iii) Continue flowing the vesicle solution into the measurement chamber for at least 5 min to ensure that the bilayer is defect free. Thereafter, wash the bilayer with Tris/NaCl no. 1 buffer at a flow rate of 100 μl min^{-1} for 5 min.

▲ CRITICAL STEP Flow the buffer constantly to check the integrity of the bilayer and wash out the adsorbed vesicles on top of the substrate. If the change in frequency value increases past −23 Hz, add additional vesicle solution to reduce potential SLB defects.

(iv) Wash again with Tris/NaCl no. 1 buffer at a flow rate of 100 μl min^{-1} for 5 min. After washing, the final resonance frequency and dissipation values should be −25 ± 1.0 Hz and less than 0.2 × 10^{-6}, respectively.

▲ CRITICAL STEP Ensure that the Tris/NaCl no. 3 buffer is exchanged with the Tris/NaCl no. 1 buffer. This will remove calcium ions from the solution and allow the SLB to have a high degree of lateral lipid diffusivity, resulting in a fluid bilayer. If calcium is still present, then the lateral lipid diffusivity within the SLB will be significantly reduced.

(C) Formation of zwitterionic SLBs on gold substrate induced by AH peptide ● **TIMING ~3 h**

(i) Repeat the procedure described above up to Step 6.

(ii) Restart the measurement and allow it to stabilize for at least 5 min. Thereafter, add a ~0.1 mg ml^{-1} POPC vesicle solution diluted in Tris/NaCl no. 1 buffer at a flow rate of 250 μl min^{-1}. After adsorption, the vesicles will remain intact on the surface instead of rupturing.

▲ CRITICAL STEP The most critical factors for forming a complete bilayer in the next step are as follows: complete coverage of intact vesicles, size distribution of vesicles (average diameter <70 nm) and eliminating excess vesicles by buffer wash. The frequency change corresponds to the average size of the vesicles and the fraction of surface coverage[84]. For E series instruments, a frequency change of −140 Hz corresponds to POPC vesicles extruded with a 30 nm polycarbonate etch-tracked membrane. For the D300 instrument, the change should be −120 Hz. The mass deviation is mainly from the flow difference of the two systems (batch versus continuous). Flow rate conditions affect how vesicles deform once absorbed onto the substrate.

(iii) Wash the adsorbed, intact vesicles with Tris/NaCl no. 1 buffer at a flow rate of 100 μl min^{-1} for 30 min to eliminate excess vesicles on top of the adsorbed vesicles as well as vesicles in solution.

▲ CRITICAL STEP It is important to eliminate excess vesicles in solution and those adsorbed onto the tubing walls. Otherwise, the residual vesicles will interact with the AH peptide and cause vesicle fusion and aggregation in solution. When using D300, wash at least four times in the 'sensor out' position.

(iv) Once the signal has stabilized, add AH peptide (13 μM) at a flow rate of 50 μl min^{-1}.

▲ CRITICAL STEP For D300, inject 1 ml with the 'sensor out' position setting and then wait for the temperature to stabilize. Add an additional 1 ml with the 'loop out' position setting and then close. Ensure that air bubbles are not introduced during solution exchange. For the E series, prepare 3 ml of the AH peptide solution and allow it to flow for 10 min or alternatively recirculate the AH peptide solution.

(v) Wait until frequency and dissipation values reach approximately −25 Hz and 0.2 × 10^{-6}, respectively. Thereafter, wash with Tris/NaCl no. 1 at a flow rate of 100 μl min^{-1} for 10 min.

● **TIMING**

Formation of SLBs on a silicon oxide substrate should take 2 h, including stabilization time. On gold and titanium oxide substrates, SLB formation, including the AH peptide-induced vesicle rupture procedure, should take a total of 4 h. Note that these times are only for the formation of SLB platforms. For example, a protein-binding study may take an additional few hours depending on the experiment of interest. In addition, vesicle preparation before the experiment will take several hours.

? TROUBLESHOOTING

To reproducibly form complete SLBs on solid substrates with QCM-D monitoring for the subsequent investigation of biomacromolecular interactions, the critical steps discussed above should be followed with care. There are two main areas of troubleshooting associated with this protocol that the critical steps address. First, SLB is a platform that can be used in conjunction with the QCM-D sensor, such as the QCM-D. Therefore, the QCM-D performance must first be verified in air and then in liquid. Analysis of QCM-D solutions in liquid follows a complex series of equations, the independent variables of which include viscosity, temperature and density. Care needs to be taken so that changes in these properties do not hinder an accurate quantitative detection of the interaction taking place on the quartz crystal substrate. After verifying the device performance, attention must be shifted to the formation of a complete SLB. The QCM-D analysis permits measurement of the adsorbed lipids' mass and viscoelastic properties. Incomplete SLB formation is not uncommon and can be easily verified by a properly operating machine. Numerous material and experimental parameters need to be carefully selected to limit abrupt changes in the physical properties of the liquid (e.g., high flow rate can cause pressure-related responses) and to favor the spontaneous adsorption and rupture of lipid vesicles onto the substrate (e.g., vesicle size and substrate conditions). Taken together, the critical steps provide a guideline to promote the self-assembly of a complete SLB, which can be verified through two important properties (i.e., mass and viscoelasticity) with QCM-D monitoring.

ANTICIPATED RESULTS

Supported lipid bilayer formation on various solid substrates including silicon oxide, titanium oxide and gold is highly reproducible when using the protocols discussed above. Regardless of the substrate and lipid composition, the SLB should exhibit similar mass and viscoelastic properties, enabling its use as a platform to investigate membrane-associated biomacromolecular interactions. Although QCM-D can probe these two physical properties in real time, thereby offering a fundamental characterization of the SLB self-assembly process, there is an increasing demand to combine QCM-D with complementary techniques for the monitoring of subsequent biomacromolecular interactions. As progress is made toward the design of increasingly sophisticated cell-membrane mimics, parallel integration of multiple techniques relying on different physical principles is likely to have a key role for elucidating new insight into the interaction kinetics and dynamics. From the SLB fabrication and characterization methods presented in this protocol, more complex biomimetic platforms can be developed and used together with the sensitive QCM-D technique. Such work shows the emerging potential at the nexus of nanobiotechnology and more traditional biological fields for improving our knowledge of fundamental biological pathways.

ACKNOWLEDGMENTS N.-J.C. is a recipient of an American Liver Foundation Postdoctoral Fellowship Award and a Global Roche Postdoctoral Fellowship. We wish to thank all the members of the Frank, Kasemo and Hook laboratories, who laid the foundation for future studies in the biomimetic sensor field.

AUTHOR CONTRIBUTIONS N.-J.C. and F.H. conceived and designed the protocol and wrote the paper; C.W.F. and B.K. contributed to data analysis and paper editing.

COMPETING FINANCIAL INTERESTS The authors declare no competing financial interests.

Published online at http://www.natureprotocols.com/.
Reprints and permissions information is available online at http://npg.nature.com/reprintsandpermissions/.

1. Sackmann, E. Supported membranes: scientific and practical applications. *Science* **271**, 43–48 (1996).
2. Tanaka, M. & Sackmann, E. Supported membranes as biofunctional interfaces and smart biosensor platforms. *Physica Status Solidi A* **203**, 3452–3462 (2006).
3. Hook, F., Kasemo, B., Grunze, M. & Zauscher, S. Quantitative biological surface science: challenges and recent advances. *ACS Nano* **2**, 2428–2436 (2008).
4. White, R.J. *et al.* Ionic conductivity of the aqueous layer separating a lipid bilayer membrane and a glass support. *Langmuir* **22**, 10777–10783 (2006).
5. White, R.J. *et al.* Single ion-channel recordings using glass nanopore membranes. *J. Am. Chem. Soc.* **129**, 11766–11775 (2007).
6. Boxer, S.G. Molecular transport and organization in supported lipid membranes. *Curr. Opin. Chem. Biol.* **4**, 704–709 (2000).
7. Kaiser, H.J. *et al.* Order of lipid phases in model and plasma membranes. *Proc. Natl. Acad. Sci. USA* **106**, 16645–16650 (2009).
8. Hook, F., Rodahl, M., Kasemo, B. & Brzezinski, P. Structural changes in hemoglobin during adsorption to solid surfaces: effects of pH, ionic strength, and ligand binding. *Proc. Natl. Acad. Sci. USA* **95**, 12271–12276 (1998).
9. Hook, F. *et al.* Variations in coupled water, viscoelastic properties, and film thickness of a Mefp-1 protein film during adsorption and cross-linking: a quartz crystal microbalance with dissipation monitoring, ellipsometry, and surface plasmon resonance study. *Anal. Chem.* **73**, 5796–5804 (2001).
10. Cho, N.J., Cheong, K.H., Lee, C., Frank, C.W. & Glenn, J.S. Binding dynamics of hepatitis C virus' NS5A amphipathic peptide to cell and model membranes. *J. Virol.* **81**, 6682–6689 (2007).
11. Cho, N.J., Cho, S.J., Cheong, K.H., Glenn, J.S. & Frank, C.W. Employing an amphipathic viral peptide to create a lipid bilayer on Au and TiO2. *J. Am. Chem. Soc.* **129**, 10050–10051 (2007).
12. Cooper, M.A. & Singleton, V.T. A survey of the 2001 to 2005 quartz crystal microbalance biosensor literature: applications of acoustic physics to the analysis of biomolecular interactions. *J. Mol. Recognit.* **20**, 154–184 (2007).
13. Kasemo, B. & Hook, F. Protein and vesicle interaction with surfaces. *Abstr. Pap. Am. Chem. Soc.* **223**, U444–U444 (2002).
14. Purrucker, O., Fortig, A., Jordan, R., Sackmann, E. & Tanaka, M. Control of frictional coupling of transmembrane cell receptors in model cell membranes with linear polymer spacers. *Phys. Rev. Lett.* **98** (2007).
15. Thid, D. *et al.* Supported phospholipid bilayers as a platform for neural progenitor cell culture. *J. Biomed. Mater. Res.* **84**, 940–953 (2008).
16. Tu, R.S. & Tirrell, M. Bottom-up design of biomimetic assemblies. *Adv. Drug Deliv. Rev.* **56**, 1537–1563 (2004).
17. Tamm, L.K. & McConnell, H.M. Supported phospholipid bilayers. *Biophys. J.* **47**, 105–113 (1985).
18. Axelrod, D., Koppel, D.E., Schlessinger, J., Elson, E. & Webb, W.W. Mobility measurement by analysis of fluorescence photobleaching recovery kinetics. *Biophys. J.* **16**, 1055–1069 (1976).

19. Richter, R., Mukhopadhyay, A. & Brisson, A. Pathways of lipid vesicle deposition on solid surfaces: a combined QCM-D and AFM study. *Biophys. J.* **85**, 3035–3047 (2003).
20. Morigaki, K. & Tawa, K. Vesicle fusion studied by surface plasmon resonance and surface plasmon fluorescence spectroscopy. *Biophys. J.* **91**, 1380–1387 (2006).
21. Reimhult, E., Larsson, C., Kasemo, B. & Hook, F. Simultaneous surface plasmon resonance and quartz crystal microbalance with dissipation monitoring measurements of biomolecular adsorption events involving structural transformations and variations in coupled water. *Anal. Chem.* **76**, 7211–7220 (2004).
22. Oxhamre, C., Richter-Dahlfors, A., Zhdanov, V.P. & Kasemo, B. A minimal generic model of bacteria-induced intracellular Ca2+ oscillations in epithelial cells. *Biophys. J.* **88**, 2976–2981 (2005).
23. Stroumpoulis, D., Parra, A. & Tirrell, M. A kinetic study of vesicle fusion on silicon dioxide surfaces by ellipsometry. *AIChE J.* **52**, 2931–2937 (2006).
24. Cho, N.J. *et al.* Alpha-helical peptide-induced vesicle rupture revealing new insight into the vesicle fusion process as monitored *in situ* by quartz crystal microbalance-dissipation and reflectometry. *Anal. Chem.* **81**, 4752–4761 (2009).
25. Wang, G. *et al.* A combined reflectometry and quartz crystal microbalance with dissipation setup for surface interaction studies. *Rev. Sci. Instrum.* **79**, 075107 (2008).
26. Anderson, T.H. *et al.* Formation of supported bilayers on silica substrates. *Langmuir* **25**, 6997–7005 (2009).
27. Kanazawa, K. & Gordon, J. The oscillation frequency of a quartz resonator in contact with a liquid. *Anal. Chim. Acta* **175**, 99–106 (1985).
28. Kanazawa, K.K. & Reed, C.E. A new description for the viscoelastically loaded quartz resonator. *Abstr. Pap. Am. Chem. Soc.* **198**, 89 Anyl (1989).
29. Rodahl, M. *et al.* Simultaneous frequency and dissipation factor QCM measurements of biomolecular adsorption and cell adhesion. *Faraday Discuss.* **107**, 229–246 (1997).
30. Rodahl, M., Hook, F. & Kasemo, B. QCM operation in liquids: an explanation of measured variations in frequency and Q factor with liquid conductivity. *Anal. Chem.* **68**, 2219–2227 (1996).
31. Rodahl, M., Hook, F., Krozer, A., Brzezinski, P. & Kasemo, B. Quartz-crystal microbalance setup for frequency and q-factor measurements in gaseous and liquid environments. *Rev. Sci. Instrum.* **66**, 3924–3930 (1995).
32. Rodahl, M. & Kasemo, B. Frequency and dissipation-factor responses to localized liquid deposits on a QCM electrode. *Sens. Actuators B Chem.* **37**, 111–116 (1996).
33. Rodahl, M. & Kasemo, B. On the measurement of thin liquid overlayers with the quartz-crystal microbalance. *Sens. Actuators A Phys.* **54**, 448–456 (1996).
34. Rodahl, M. & Kasemo, B. A simple setup to simultaneously measure the resonant frequency and the absolute dissipation factor of a quartz crystal microbalance. *Rev. Sci. Instrum.* **67**, 3238–3241 (1996).
35. Cho, N.J., Kanazawa, K.K., Glenn, J.S. & Frank, C.W. Employing two different quartz crystal microbalance models to study changes in viscoelastic behavior upon transformation of lipid vesicles to a bilayer on a gold surface. *Anal. Chem.* **79**, 7027–7035 (2007).
36. Hook, F. & Kasemo, B. The QCM-D technique for probing biomacromolecular recognition reactions. *Springer Ser. Chem. Sens. Biosens.* **5**, 425–447 (2007).
37. Keller, C.A. & Kasemo, B. Surface specific kinetics of lipid vesicle adsorption measured with a quartz crystal microbalance. *Biophys. J.* **75**, 1397–1402 (1998).
38. Keller, C.A., Glasmastar, K., Zhdanov, V.P. & Kasemo, B. Formation of supported membranes from vesicles. *Phys. Rev. Lett.* **84**, 5443–5446 (2000).
39. Lee, S.E. *et al.* Biologically functional cationic phospholipid-gold nanoplasmonic carriers of RNA. *J. Am. Chem. Soc.* **131**, 14066–14074 (2009).
40. Larsson, E.M., Edvardsson, M.E., Langhammer, C., Zoric, I. & Kasemo, B. A combined nanoplasmonic and electrodeless quartz crystal microbalance setup. *Rev. Sci. Instrum.* **80**, 125105 (2009).
41. Jonsson, M.P., Jonsson, P. & Hook, F. Simultaneous nanoplasmonic and quartz crystal microbalance sensing: analysis of biomolecular conformational changes and quantification of the bound molecular mass. *Anal. Chem.* **80**, 7988–7995 (2008).
42. Jonsson, M.P., Jonsson, P., Dahlin, A.B. & Hook, F. Supported lipid bilayer formation and lipid-membrane-mediated biorecognition reactions studied with a new nanoplasmonic sensor template. *Nano Lett.* **7**, 3462–3468 (2007).
43. Misra, N. *et al.* Bioelectronic silicon nanowire devices using functional membrane proteins. *Proc. Natl Acad. Sci. USA* **106**, 13780–13784 (2009).
44. Kasemo, B. & Lausmaa, J. Material-tissue interfaces: the role of surface properties and processes. *Environ. Health Perspect.* **102** (Suppl 5): 41–45 (1994).
45. Seifert, U., Berndl, K. & Lipowsky, R. Shape transformations of vesicles—phase-diagram for spontaneous-curvature and bilayer-coupling models. *Phys. Rev. A* **44**, 1182–1202 (1991).
46. Shillcock, J.C. & Lipowsky, R. Tension-induced fusion of bilayer membranes and vesicles. *Nat. Mater.* **4**, 225–228 (2005).
47. Polozov, I.V., Anantharamaiah, G.M., Segrest, J.P. & Epand, R.M. Osmotically induced membrane tension modulates membrane permeabilization by class L amphipathic helical peptides: nucleation model of defect formation. *Biophys. J.* **81**, 949–959 (2001).
48. Lasic, D.D. The mechanism of vesicle formation. *Biochem. J.* **256**, 1–11 (1988).
49. Lasic, D.D. & Martin, F.J. On the mechanism of vesicle formation. *J. Memb. Sci.* **50**, 215–222 (1990).
50. Watwe, R.M. & Bellare, J.R. Manufacture of liposomes—a review. *Curr. Sci.* **68**, 715–724 (1995).
51. Winterhalter, M. & Lasic, D.D. Liposome stability and formation—experimental parameters and theories on the size distribution. *Chem. Phys. Lipids* **64**, 35–43 (1993).
52. Armengol, X. & Estelrich, J. Physical stability of different liposome compositions obtained by extrusion method. *J. Microencapsul.* **12**, 525–535 (1995).
53. Shingles, R. & McCarty, R.E. Production of membrane vesicles by extrusion: size distribution, enzyme activity, and orientation of plasma membrane and chloroplast inner-envelope membrane vesicles. *Anal. Biochem.* **229**, 92–98 (1995).
54. Seantier, B. & Kasemo, B. Influence of mono- and divalent ions on the formation of supported phospholipid bilayers via vesicle adsorption. *Langmuir* **25**, 5767–5772 (2009).
55. Kasemo, B. Biocompatibility of titanium implants: surface science aspects. *J. Prosthet. Dent.* **49**, 832–837 (1983).
56. Kasemo, B. & Lausmaa, J. Aspects of surface physics on titanium implants. *Swed. Dent. J. Suppl.* **28**, 19–36 (1985).
57. Greve, F. *et al.* Molecular design and characterization of the neuron-microelectrode array interface. *Biomaterials* **28**, 5246–5258 (2007).
58. Reimhult, E., Hook, F. & Kasemo, B. Vesicle adsorption on SiO2 and TiO2: Dependence on vesicle size. *J. Chem. Phys.* **117**, 7401–7404 (2002).
59. Modin, C. *et al.* QCM-D studies of attachment and differential spreading of pre-osteoblastic cells on Ta and Cr surfaces. *Biomaterials* **27**, 1346–1354 (2006).
60. Ekeroth, J., Konradsson, P. & Höök, F. Bivalent-ion-mediated vesicle adsorption and controlled supported phospholipid bilayer formation on molecular phosphate and sulfate layers on gold. *Langmuir* **18**, 7923–7929 (2002).
61. Rossetti, F.F., Textor, M. & Reviakine, I. Asymmetric distribution of phosphatidyl serine in supported phospholipid bilayers on titanium dioxide. *Langmuir* **22**, 3467–3473 (2006).
62. Rossetti, F.F., Bally, M., Michel, R., Textor, M. & Reviakine, I. Interactions between titanium dioxide and phosphatidyl serine-containing liposomes: formation and patterning of supported phospholipid bilayers on the surface of a medically relevant material. *Langmuir* **21**, 6443–6450 (2005).
63. Kunze, A., Sjovall, P., Kasemo, B. & Svedhem, S. *In situ* preparation and modification of supported lipid layers by lipid transfer from vesicles studied by QCM-D and TOF-SIMS. *J. Am. Chem. Soc.* **131**, 2450–2451 (2009).
64. Jackman, J.A., Cho, N.J., Duran, R.S. & Frank, C.W. Interfacial binding dynamics of bee venom phospholipase A(2) investigated by dynamic light scattering and quartz crystal microbalance. *Langmuir* **26**, 4103–4112 (2010).
65. Cho, N.J. *et al.* Quartz resonator signatures under Newtonian liquid loading for initial instrument check. *J. Colloid Interface Sci.* **315**, 248–254 (2007).
66. Reimhult, E., Hook, F. & Kasemo, B. Temperature dependence of formation of a supported phospholipid bilayer from vesicles on SiO2. *Phy. Rev. E* **66** (2002).
67. Reimhult, E., Hook, F. & Kasemo, B. Intact vesicle adsorption and supported biomembrane formation from vesicles in solution: Influence of surface chemistry, vesicle size, temperature, and osmotic pressure. *Langmuir* **19**, 1681–1691 (2003).
68. Zhdanov, V.P., Dimitrievski, K. & Kasemo, B. Adsorption and spontaneous rupture of vesicles composed of two types of lipids. *Langmuir* **22**, 3477–3480 (2006).

69. Dimitrievski, K., Reimhult, E., Kasemo, B. & Zhdanov, V.P. Simulations of temperature dependence of the formation of a supported lipid bilayer via vesicle adsorption. *Colloids Surf. B Biointerfaces* **39**, 77–86 (2004).
70. Dimitrievski, K. & Kasemo, B. Influence of lipid vesicle composition and surface charge density on vesicle adsorption events: a kinetic phase diagram. *Langmuir* **25**, 8865–8869 (2009).
71. Sauerbrey, G. Verwendung von Schwingquarzen zur Wagung dunner Schichten und zur Mikrowagung. *Z. Phys.* **155**, 206–222 (1959).
72. Voinova, M.V., Rodahl, M., Jonson, M. & Kasemo, B. Viscoelastic acoustic response of layered polymer films at fluid-solid interfaces: continuum mechanics approach. *Phys. Scr.* **59**, 391–396 (1999).
73. Johannsmann, D., Reviakine, I. & Richter, R.P. Dissipation in films of adsorbed nanospheres studied by quartz crystal microbalance (QCM). *Anal. Chem.* **81**, 8167–8176 (2009).
74. Richter, R.P. & Brisson, A.R. Following the formation of supported lipid bilayers on mica: a study combining AFM, QCM-D, and ellipsometry. *Biophys. J.* **88**, 3422–3433 (2005).
75. Kasemo, B. & Lausmaa, J. Biomaterial and implant surfaces: on the role of cleanliness, contamination, and preparation procedures. *J. Biomed. Mater. Res.* **22** (A2 Suppl): 145–158 (1988).
76. Hook, F. *et al.* A comparative study of protein adsorption on titanium oxide surfaces using *in situ* ellipsometry, optical waveguide lightmode spectroscopy, and quartz crystal microbalance/dissipation. *Colloids Surf. B Biointerfaces* **24**, 155–170 (2002).
77. Mashaghi, A., Swann, M., Popplewell, J., Textor, M. & Reimhult, E. Optical anisotropy of supported lipid structures probed by waveguide spectroscopy and its application to study of supported lipid bilayer formation kinetics. *Anal. Chem.* **80**, 3666–3676 (2008).
78. Richter, R.P., Maury, N. & Brisson, A.R. On the effect of the solid support on the interleaflet distribution of lipids in supported lipid bilayers. *Langmuir* **21**, 299–304 (2005).
79. Stelzle, M. & Sackmann, E. Sensitive detection of protein adsorption to supported lipid bilayers by frequency-dependent capacitance measurements and microelectrophoresis. *Biochim. Biophys. Acta.* **981**, 135–142 (1989).
80. Cho, N.J., Cho, S.J., Hardesty, J.O., Glenn, J.S. & Frank, C.W. Creation of lipid partitions by deposition of amphipathic viral peptides. *Langmuir* **23**, 10855–10863 (2007).
81. Meyvis, T.K., De Smedt, S.C., Van Oostveldt, P. & Demeester, J. Fluorescence recovery after photobleaching: a versatile tool for mobility and interaction measurements in pharmaceutical research. *Pharm. Res.* **16**, 1153–1162 (1999).
82. Bailey, L.E. *et al.* Multistep adsorption of perfluoropolyether hard-disk lubricants onto amorphous carbon substrates from solution. *Langmuir* **17**, 8145–8155 (2001).
83. Bobardt, M.D. *et al.* Hepatitis C virus NS5A anchor peptide disrupts human immunodeficiency virus. *Proc. Natl Acad. Sci. USA* **105**, 5525–5530 (2008).
84. Cho, N.J. *et al.* The mechanism of an amphipathic α-helical peptide's antiviral activity involves size-dependent virus particle lysis. *ACS Chem. Biol.* **4**, 1061–1067 (2009).
85. Han, X. *et al.* Supported bilayer lipid membrane arrays on photopatterned self-assembled monolayers. *Chemistry* **13**, 7957–7964 (2007).
86. Purrucker, O. *et al.* Polymer-tethered membranes as quantitative models for the study of integrin-mediated cell adhesion. *Soft Matter* **3**, 333–336 (2007).
87. Sklan, E.H. *et al.* A Rab-GAP TBC domain protein binds hepatitis C virus NS5A and mediates viral replication. *J. Virol.* **81**, 11096–11105 (2007).
88. Yu, X. *et al.* Cryo-electron microscopy and three-dimensional reconstructions of hepatitis C virus particles. *Virology* **367**, 126–134 (2007).